Int J Adv Manuf Technol (2013) 69:93–106
DOI 10.1007/s00170-013-5007-9

ORIGINAL ARTICLE

Experimental investigation on submerged arc welding of Cr–Mo–V steel

R. Venkata Rao · V. D. Kalyankar

Received: 12 June 2012 / Accepted: 8 April 2013 / Published online: 24 April 2013

Abstract Welding aspects of a high-quality Cr–Mo–V steel are investigated in the present work. Cr–Mo–V steel can be suggested as a best choice for fabrication of pressure vessels to be operated in high-temperature operating conditions. Welding of this group of steel demands very critical attention on the parameters setting of chosen welding process. Only a few researchers had carried out research on the optimization aspects of the submerged arc welding of Cr–Mo–V steel. In the present work, complete experimental analysis is carried out on the submerged arc welding of Cr–Mo–V steel. The important input process parameters considered are welding current, voltage, welding speed, and wire feed. The effect of these input parameters is studied on various responses related to weld bead geometry and few mechanical properties. Taguchi's L_9 orthogonal array is used for design of experiment and the mathematical models are developed for the responses using MINITAB 15 software. The models developed are validated by conducting more experiments. Optimised parameter setting is also obtained by using a recently developed teaching–learning-based optimization algorithm.

Keywords Cr–Mo–V steel · Submerged arc welding · Process parameters · Teaching–learning-based optimization algorithm

1 Introduction

The welding of heavy steel sections are subjected to various difficulties such as distortion, residual stress, softening and hardening of heat-affected zone of steel because most of the steels are structure sensitive. In the present competitive scenario, the major efforts of the designers and manufacturers are to raise the thermal efficiency of advanced power generation systems and other similar products. This can be achieved if the process under consideration is operated at higher operating temperatures and pressures. Ordinary steel cannot sustain its properties at high-operating conditions and hence designers are shifting towards the use of new constructional materials having improved high-temperature properties. The family of Cr–Mo steels is one of the best heat-resisting materials which can be used to fabricate the components for pressure vessels, power systems, nuclear, chemical, food processing and petroleum industries.

The modified Cr–Mo steel is a heavy-duty material and can be used in the fabricating industries because of its good creep resistance property. It gives excellent strength and toughness at low temperatures and has elevated temperature creep resistance in combination with good corrosion resistance. The elevated-temperature properties make this steel economically attractive compared to the presently used austenitic stainless steels and high-nickel alloys up to about 600 °C. Welding of such a refractory materials demands high heat input. Submerged arc welding (SAW) is mostly preferred in fabricating industries due to its higher heat input and higher deposition rate with better bead characteristics. Submerged arc welding also becomes one of the cost-effective means of getting strong weld joint by selecting proper process control parameters and hence may be considered for welding of modified Cr–Mo steel.

The literature survey shows some research-oriented work on the welding of Cr–Mo category of steels out of which the important works are presented below which are in the direction of present work. Swindeman et al. [1] discussed various issues related to replacement of Cr–Mo steels and stainless steels with 9Cr–1Mo–V steel. Various advantages of Cr–Mo–V steel were presented in their work over the other steels. Lu et al. [2] carried out the cladding on Cr–Mo–V steel using submerged arc welding process and discussed

R. V. Rao (✉) · V. D. Kalyankar
Department of Mechanical Engineering,
S. V. National Institute of Technology, Surat 395007, India
e-mail: ravipudirao@rediffmail.com

the effects on microstructure and wear properties of welded material. Storesund et al. [3] carried out the inspection on X-20-CrMoV-12-1 steel welding and simulated the creep behaviour of welded parts. Zielinski et al. [4] studied the structural changes in low alloy cast Cr–Mo–V steel to investigate the creep behaviour of the material. Prasad and Dwivedi [5] carried out submerged arc welding of HSLA steel and investigated the microstructure and mechanical properties of welded joints. Hilkes and Gross [6] discussed the past, present and future of Cr–Mo steel welding and its application for power generation and petrochemical industries. Naz et al. [7] carried out the failure analysis of low carbon Cr–Mo–V steel weldment by inspecting the crack formation in heat-affected zone area. Arivazhagan et al. [8] used 9Cr–1Mo steel and focused their research on weld fusion zone to study the microstructure and mechanical properties of welded parts. Babu and Natarajan [9] studied the corrosion and characterization aspects of flux cored arc welded 2.25Cr–1Mo steel used in power plants.

Few researchers had carried out the experimental work in the past to study the effect of various input variables of submerged arc welding for various grades of steel [10–15]. Optimization aspects of submerged arc welding process were also reported in the past [16–20], and genetic algorithm [19, 20] and particle swarm optimization [20] techniques were used for optimization of the process parameters of submerged arc welding. Use of Taguchi method was also observed in the past for carrying out the parameters optimization of submerged arc welding process [21–25].

The aim of this work is to understand the influence of SAW process parameters on the welding of Cr–Mo–V steel plate through experimentation. In the present work, 9Cr–1Mo steel with 0.2 % vanadium is investigated. The welding of this Cr–Mo–V steel is successfully carried out and the effect of various important input parameters is studied on the weld bead geometry and mechanical properties of the material. The SAW process involves various input parameters and determination of optimum process parameters is very important in SAW process. Hence, generalised mathematical models are also developed for various responses which will be very useful for determining the optimum parameter setting. The complete experimental work is explained in detail in Section 2.

2 Experimental details

The automatic SAW process for welding of Cr–Mo–V steels demands attention on various aspects before beginning of the welding. In this work, various aspects starting from selection of SAW wire and flux up to the test specimen preparation are carefully handled and these are explained in the following subsections.

2.1 Variables considered

The SAW process consists of several input variables out of which few variables show very significant effect on the output of the process. After thorough literature survey, the important input variables considered in the present work are welding current (I), voltage (V), welding speed (S) and wire feed (F). Initially, trail experiments have been conducted on the Cr–Mo–V steel under consideration to decide the variables range and their levels and, finally, three levels are decided as shown in Table 1.

2.2 Design of experiments

Conducting experiments by considering each variable at all the three levels is a very costly affair as well as very time consuming. Hence, in order to limit the total number of experiments in the present work, the Taguchi's L_9 orthogonal array is used for four variables with three levels. Similar orthogonal array was also reported by many researchers in their experimental work of SAW process on certain types of steels as well as for other manufacturing processes [20–25]. By using Taguchi's L_9 orthogonal array in the present work, the total number of experiments to be conducted is nine and the detailed design of experiments is given in Table 2.

2.3 Material composition

Cr–Mo–V steel plate which is more suitable for fabrication of heavy-duty products under high-temperature operating condition is considered in the present work. A material with trade name as SA387 grade 91 class 2 is chosen with plate thickness as 11 mm. It is one among the modified group of Cr–Mo steels. The chemical composition of the material used for the present research work is given in Table 3. The material was normalised at 1,050 °C and tempered at 770 °C during its fabrication stage and the entire plate was ultrasonically tested by the supplier.

2.4 SAW wire and flux composition

The selection of appropriate SAW wire and flux is very important stage for SAW process to obtain good weld joint

Table 1 Input variables and their levels

Parameter	Unit	Levels		
		−1	0	+1
Current (I)	Amp	350	400	450
Voltage (V)	V	28	30	32
Welding speed (S)	cm/min	4	12	20
Wire feed (F)	cm/min	190	250	310

Table 2 Design of experiments

Expt no.	*I* (Amp)	*V* (volts)	*S* (cm/min)	*F* (cm/min)
1	350	28	4	190
2	350	30	12	250
3	350	32	20	310
4	400	28	12	310
5	400	30	20	190
6	400	32	4	250
7	450	28	20	250
8	450	30	4	310
9	450	32	12	190

with significant properties. The composition of wire and flux should be such that it should match the overall chemistry of the weld joint. Overall matching consumables are required for the welding of Cr–Mo–V steel plates in order to achieve homogenous and strong weld joint [6]. Keeping in view the various problems involved with the welding of modified Cr–Mo steel, a 3.00 mm low-alloyed, copper-coated ESAB make wire is selected. The wire is designed for the submerged arc welding of creep-resistant Cr–Mo group of steels. The wire was coded by the manufacturer as OK AUTROD 13.20 (EB-3-21/4Cr1Mo) with electrode classification as AWS A5.23: EB3R.

The ESAB make agglomerated fluoride basic flux suitable for submerged arc welding of Cr–Mo group of steels and best suitable for OK AUTROD 13.20 wire is selected. The flux was coded by the manufacturer as OK FLUX 10.62 and the grain size of the flux used varies from 0.2 to 1.6 mm. The flux is preheated every time before conducting any experiment to reduce the chances of defects.

2.5 SAW machine specification

A 600-Amp thyristorised controlled automatic submerged arc welding machine with tractor-mounted welding head fitting is used to conduct all the welding experiments. The recommended input supply for the machine is 415 V, three phases and 50 Hz. The welding speed varies from 0 to 150 cm/min and the wire feed range varies from 50 to 450 cm/min.

2.6 Specimen preparation

A number of specimens are prepared in the plate form of the size of 200×100×11 mm. Edge preparation is done by providing a 30° bevel on one side of the plate so that when two plates with bevel edge brought in contact with each other, then a butt joint of ‘V’ shape can be formed. The edges to be welded are cleaned properly in order to ensure a dirt-free surface (Fig. 1).

Two plates with butt joint are then clamped together with the help of ‘C’ clamp and the assembly is then preheated for approximately 30 min and the flux is also preheated. With this, the atmospheric effect is minimised and chances of weld defects are also reduced. Assembly of one such setup is shown in Fig. 2.

2.7 Welding of specimens

The specimen assembly as shown in Fig. 2 is preheated along with the flux before the start of welding. The input variables are adjusted on the SAW machine as per the design of experiment for respective experiments. A very careful adjustment is required for the direction of trolley travel so that the wire feeding should be exactly at the centre of V joint. This is because, as the welding proceeds, the steel plates may distort due to large amount of heat. Hence, for this purpose, proper clamping arrangement is provided for the weld joint. In the present work, all the nine experiments are conducted very carefully in order to achieve good quality and defect-free weld joint for all the experiments. One of the welded plates of the present experiment is shown in Fig. 3 to visualise the appearance of weld joint.

2.8 Post-weld preparation for testing and analysis

After completion of welding, each specimen is subjected to post-weld heat treatment in the furnace in order to improve the mechanical properties. All the weld joints are then needed to be prepared for analysis by measuring various outputs obtained from each experiment. In the present work, various outputs considered for analysis purpose are weld bead width, weld reinforcement, weld penetration, weld tensile strength and weld hardness. To prepare the test sample, some welded portion is removed by cutting it form the portion marked as shown in Fig. 3. For measuring the weld bead geometry and hardness, a specimen of 20-mm width is removed from the centre of weld joint of each plate and it is directly used for the measurement purpose. For tensile strength measurement, separate portion of 50 mm width is removed from which a tensile test specimen is prepared as per the ASTM E8 standard. Figure 4 shows various test samples prepared from each experiment for conducting different tests.

Table 3 Chemical composition of the material

C	Cr	Mo	V	Al	Nb	Zr	Ti	Ni	Mn	P	S
0.105	8.975	0.855	0.202	0.013	0.075	0.006	0.002	0.228	0.432	0.014	0.0008

Fig. 1 Submerged arc welding machine

3 Results and discussion

After conducting all the experiments, various responses are measured accurately and the effect of all input variables on each response is then analysed to identify the critical variables affecting the various responses. Various outputs variables considered in this work are: weld bead width, weld reinforcement, weld penetration, weld tensile strength and weld hardness. For measuring each of these responses, sophisticated equipments are used having high degree of accuracy. The various equipments used to carry out different tests are: Toolmakers' microscope for measuring weld bead width and reinforcement, digital vernier calliper for measuring weld penetration, universal testing machine of capacity 1,000 kN for measuring weld tensile strength and Rockwell hardness tester for measuring weld hardness. Before conducting all the tests and measurements, trials have been conducted to ensure the smooth functioning of respective

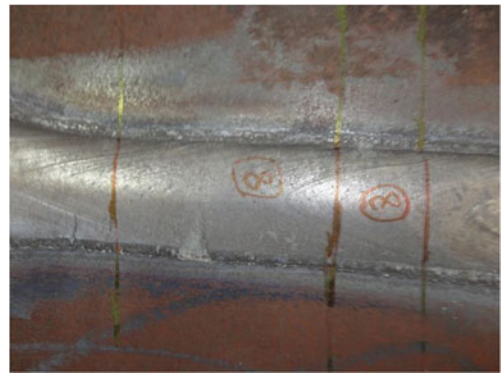

Fig. 3 Welded specimen after experiment

equipment. The results obtained for each response are explained below with their analysis.

3.1 Effect of process parameters on weld bead width

The weld bead width obtained for all the experiments is measured by using the Toolmakers's microscope having a least count of 0.001 mm. Fine setting of the lens is maintained in order to observe the clear image on the screen. A total of four readings are taken from both sides and finally average bead width is considered for each specimen. The results obtained are given in Table 4.

The bead width obtained for each experiment is analysed to check the effect of each input variable on the bead width. MINITAB 15 software is used to carry out the analysis of each response. Figure 5 shows the effect of input process variables on the bead width whereas Table 5 gives the response table for means.

The term delta in Table 5 represents the difference between the highest and lowest response for respective input variable and based on this difference the rank is decided. As

Fig. 2 Specimens used for welding with their assembly

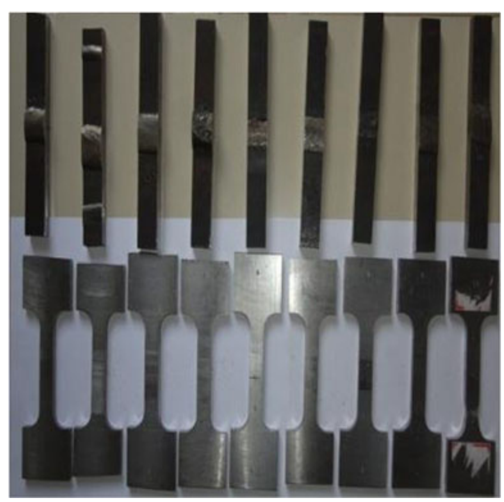

Fig. 4 Various samples prepared from each welded specimens

Table 4 Average weld bead width obtained in different experiments

Expt no.	*I* (Amp)	*V* (volts)	*S* (cm/min)	*F* (cm/min)	Weld bead width (mm)
1	350	28	4	190	26.168
2	350	30	12	250	30.969
3	350	32	20	310	29.330
4	400	28	12	310	31.354
5	400	30	20	190	18.502
6	400	32	4	250	22.025
7	450	28	20	250	19.216
8	450	30	4	310	26.259
9	450	32	12	190	29.505

the expected bead width of the weld should be minimum, hence, smaller-the-better approach is used for the analysis purpose. As observed from Fig. 5, the bead width drastically decreases as the current increases initially up to certain limit and then it shows small amount of increase in bead width if the current is further increased. In the case of voltage, the bead width remains almost constant from 28 to 30 V and afterwards shows slight increase in the bead width with the increase in voltage. It is observed that welding speed is the most significant variable affecting the bead width. It shows a sudden variation in the bead width due to change in welding speed. In case of wire feed rate, the weld bead width is not affected much up to 250 cm/min and then increased suddenly as the wire feed rate increases.

Regression analysis of the obtained result is carried out to establish the relationship between the variables. The estimated coefficients for weld bead width are obtained by using response surface modelling. Various models are attempted like only linear, linear with interaction effects, linear and square terms, full quadratic, etc. All the necessary tests to find out the coefficient of determination for each model are carried out. The coefficient of determination (R^2) is used for the prediction of future outcomes on the basis of related information between the variables. From various models, the full quadratic model given by Eq. 1 in coded form is finalised which gives better coefficient of determination (R^2).

$$\begin{aligned}\text{Bead width} = {} & 26.1070 - 1.9145(\text{I}) + 0.6870(\text{V}) \\ & - 1.2340(\text{S}) + 2.1280(\text{F}) \\ & + 2.9475(\text{I})^2 + 1.0230(\text{V})^2 \\ & - 7.0260(\text{S})^2 + 2.7830(\text{F})^2 \end{aligned} \tag{1}$$

The equation for weld bead width in uncoded form is given by Eq. 2.

$$\begin{aligned}\text{Bead width} = {} & 475.425 - 0.9814(\text{I}) - 15.0015(\text{V}) \\ & + 2.4805(\text{S}) - 0.351(\text{F}) \\ & + 0.001179(\text{I})^2 + 0.25575(\text{V})^2 \\ & - 0.109781(\text{S})^2 + 0.000773(\text{F})^2 \end{aligned} \tag{2}$$

Fig. 5 Effect of input process variable on weld bead width

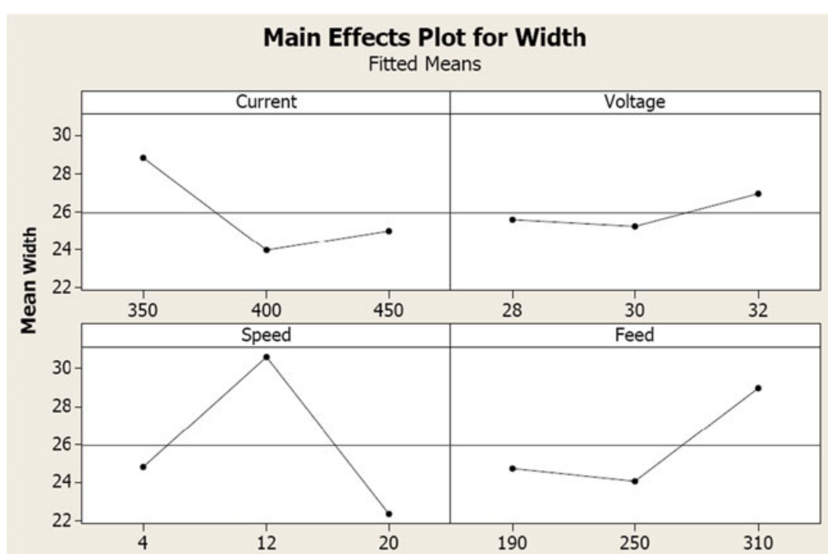

Table 5 Response table for means of bead width

Level	Mean weld bead width (mm)			
	I	*V*	*S*	*F*
−1	28.82	25.58	24.82	24.73
0	23.96	25.24	30.61	24.07
+1	24.99	26.95	22.35	28.98
Delta	4.86	1.71	8.26	4.91
Rank	3	4	1	2

R^2 obtained is 87.82 % which is very significant and hence the model either in coded form or uncoded form can be used to obtain the weld bead width using different combinations of input variables.

3.2 Effect of process parameters on weld reinforcement

Similar to weld bead width, the weld reinforcement obtained for each set is also measured using the Toolmaker's microscope. Four readings are taken for each experiment and the average reinforcement is considered. The results obtained for each experiment are given in Table 6.

It is observed that there is a significant variation in the reinforcement in the range of 0.256 to 9.46 mm. The reinforcement obtained for each experiment is analysed to check the effect of each variable on the weld reinforcement. Figure 6 shows the effect of variables on the reinforcement whereas Table 7 gives the response table for mean reinforcement.

For economic reason, the weld reinforcement should be minimum provided that the desired strength is achieved in the weld joint. Hence, smaller-the-better approach is used for the weld reinforcement analysis. From the main effects plot shown in Fig. 6, it is observed that out of the four input variables, the reinforcement consistently decreases as the welding current increases. In case of voltage, reinforcement obtained is high in the range of above 5 mm at the low level of voltage and it decreases below 3 mm as the voltage increases from 28 to 30 V. But the reinforcement again starts increasing as the voltage increases above 30 V.

Similar to weld bead width, the welding speed is observed as the most critical variable in case of weld reinforcement. For the middle level, highest mean reinforcement of above 6 mm is obtained and then it drastically decreases below 1 mm as the welding speed increases to its higher level. Wire feed rate also shows varying effect on weld reinforcement.

The regression analysis for the obtained results of weld reinforcement is carried out using response surface modelling. The best model obtained for weld reinforcement is obtained by using the combined model of linear and interaction effect having the R^2 value of 99.96 %. The model obtained for weld reinforcement in the coded form is given by Eq. 3.

$$\begin{aligned}\text{Weld reinforcement} = 3.7189 &- 0.7332(\mathrm{I}) \\ &+ 0.8908(\mathrm{V}) + 3.2839(\mathrm{S}) \\ &+ 6.6893(\mathrm{F}) + 7.7851(\mathrm{I}\times\mathrm{V}) \\ &+ 3.3659(\mathrm{I}\times\mathrm{S}) \\ &- 0.2747(\mathrm{V}\times\mathrm{S})\end{aligned} \tag{3}$$

The equation in the uncoded form for weld reinforcement is given by Eq. 4.

$$\begin{aligned}\text{Reinforcement} = 931.851 &- 2.45118(\mathrm{I}) \\ &- 30.4892(\mathrm{V}) - 2.44028(\mathrm{S}) \\ &+ 0.111489(\mathrm{F}) \\ &+ 0.0778514(\mathrm{I}\times\mathrm{V}) \\ &+ 0.00841464(\mathrm{I}\times\mathrm{S}) \\ &- 0.0171696(\mathrm{V}\times\mathrm{S})\end{aligned} \tag{4}$$

The estimated regression coefficients in the coded form along with the test result obtained from MINITAB 15 software is given in Table 8 and the ANOVA result is given in Table 9.

Table 6 Average weld reinforcement obtained in different experiments

Expt no.	*I* (Amp)	*V* (volts)	*S* (cm/min)	*F* (cm/min)	Weld reinforcement (mm)
1	350	28	4	190	4.450
2	350	30	12	250	4.567
3	350	32	20	310	3.876
4	400	28	12	310	9.46
5	400	30	20	190	0.256
6	400	32	4	250	1.543
7	450	28	20	250	1.263
8	450	30	4	310	3.054
9	450	32	12	190	5.001

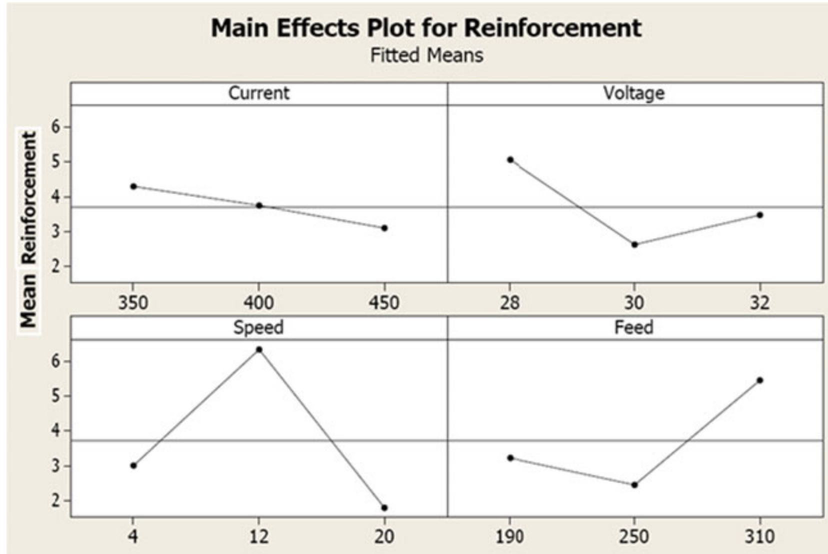

Fig. 6 Effect of input process variables on weld reinforcement

From Tables 8 and 9, it is clear that the coefficient of determination obtained for the model is almost 100 %. Hence, the equation can be satisfactorily used to obtain the weld reinforcement using different combinations of input variables with almost 100 % prediction.

3.3 Effect of process parameters on weld penetration

To achieve a good weld joint, the filler material should fuse with the base material and should penetrate at much as possible towards the root gap of weld joint. An attempt is made in the present work to obtain the maximum penetration. As the parameter setting is done as per the design of experiment hence different amount of penetration is obtained in each experiment. Measurement of the weld penetration is done through the cross-section of weld joint. A high level of surface finish is obtained on the cross-sectional area of weld joint by machining and polishing. In order to have the appearance of welded portion on the entire surface, appropriate etchant needs to be applied on the surface. For different groups of materials, different etchants are required and hence after thorough literature survey, it is concluded that 20 % nitric acid, 5 % phosphoric acid mixed with water is the best choice as an etchant for the Cr–Mo–V steel [26].

Table 7 Response table for means of weld reinforcement

Level	Mean weld reinforcement (mm)			
	I	*V*	*S*	*F*
−1	4.298	5.058	3.016	3.236
0	3.753	2.626	6.343	2.458
+1	3.106	3.473	1.798	5.463
Delta	1.192	2.432	4.544	3.006
Rank	4	3	1	2

Due to application of etchant on the cross-sectional area of welded joint, the welded portion is appeared in reddish brown colour. Figure 7 shows appearance of different weld bead geometry obtained in the present work.

The penetration obtained on each sample is measured by using digital vernier calliper having a least count of 0.01 mm. Table 10 shows the results for the weld penetration obtained for different sets of experiments.

It is observed that good penetration is obtained for all the experiments based on the parameter settings of each experiment and complete penetration is observed in case of three samples. The penetration obtained for each experiment is analysed to check the effect of each variable on the weld penetration. Figure 8 shows the effect of each variable on the weld penetration whereas Table 11 gives the response table for means based on weld penetration.

As maximum penetration is preferred to achieve maximum strength, hence larger-the-better approach is used for analysis of weld penetration. Figure 8 shows that, for the chosen sets of experiments, weld penetration goes on increasing considerably as the welding current increases. This is due to large amount of heat available due to more current and hence significant melting of material takes place to have down flow of molten metal towards root gap. Voltage is proved as the most critical variable for weld penetration because of sudden variation in the penetration from low to high and then again low penetration is observed as the voltage goes on increasing. For the lower and higher levels of voltage, comparatively less penetration is obtained and at the middle level, the highest penetration is observed, i.e. complete penetration of 11 mm for all the experiments comprising voltage of 30 V.

Using the experimental results, the full quadratic model is developed for weld penetration. Equation 5 gives the full

Table 8 Estimated regression coefficients for weld reinforcement in the coded form

Term	Coef	SE Coef	*T*	*P*
Constant	3.7189	0.05375	69.190	0.009
Current	−0.7332	0.09952	−7.367	0.086
Voltage	0.8908	0.12441	7.160	0.088
Speed	3.2839	0.12441	26.397	0.024
Feed	6.6893	0.17417	38.408	0.017
Current*Voltage	7.7851	0.21112	36.875	0.017
Current×speed	3.3659	0.21112	15.943	0.040
Voltage×speed	−0.2747	0.14929	−1.840	0.317
R^2=99.96 %	R^2 (predicted)=83.62 %		R^2 (adjusted)=99.65 %	

quadratic model in the coded form obtained by using response surface modelling.

$$\begin{aligned}\text{Weld penetration} = {} & 12.2667 + 1.0367(\text{I}) \\ & + 0.0767(\text{V}) + 0.2583(\text{S}) \\ & - 0.1450(\text{F}) - 0.23(\text{I})^2 \\ & - 2.87(\text{V})^2 - 1.185(\text{S})^2 \\ & - 0.485(\text{F})^2 \end{aligned} \tag{5}$$

The equation in the uncoded form for weld penetration is given by Eq. 6.

$$\begin{aligned}\text{Weld penetration} = {} & -668.516 + 0.094333(\text{I}) \\ & + 43.0883(\text{V}) + 0.47667(\text{S}) \\ & + 0.064944(\text{F}) - 0.000092(\text{I})^2 \\ & - 0.7175(\text{V})^2 - 0.018515(\text{S})^2 \\ & - 0.000134(\text{F})^2 \end{aligned} \tag{6}$$

Various tests are carried out on the weld penetration model and the R^2 obtained for the model is 82.3 %. The equation can be used to obtain the weld penetration using different combinations of input variables.

3.4 Effect of process parameters on tensile strength

The tensile strength of a material represents the load-bearing capacity of a material before its fail. In case of weld joint, the desired tensile strength should be achieved, because there are chances that the weld joint may have less strength due to presence of weld defects. Hence, in the present work, tensile strength is considered as one of the major responses. To carry out the tensile test of all the weld joints, all the test samples are prepared as per the ASTM standard. A computerised universal tensile testing machine having capacity of 1,000 kN is used to carry out the tensile test of all the specimens. Before carrying out the tests, all the dimensions are measured carefully at different locations of samples using digital vernier calliper. A gauge length is also marked on the sample as per the standard. The test is performed with a constant load rate of 0.05 kN/s and a strain rate of 0.10–0.20 mm/min. Fracture is observed within the gauge length but away from the weld joint which is a good indication. The change in dimension is again measured in order to get the output of the test. One of the tensile test samples before and after the tensile test is shown below in Fig. 9.

For the specimen shown in Fig. 9, a significant tensile strength of 854 MPa is obtained and the fracture occurs away from the weld joint. This is the indication of very good and strong weld joint obtained during the process. In the similar manner, tests on all other samples are carried out and the results obtained are given in Table 12.

It is observed that very good tensile strength is obtained in all the cases. The tensile strength obtained for each experiment is analysed to check the effect of each variable on the tensile strength. Figure 10 shows the effect of variables on the tensile strength whereas Table 13 gives the response table for means obtained for weld tensile strength.

As seen from the main effects plot obtained for tensile strength shown in Fig. 10, welding current is considered as

Table 9 ANOVA results for weld reinforcement

Source	DF	Seq SS	Adj SS	Adj MS	*F*	*P*
Regression	7	59.0562	59.0562	8.4366	324.47	0.043
Linear	4	15.5619	48.9472	12.2368	470.63	0.035
Interaction	3	43.4944	43.4944	14.4981	557.60	0.031
Residual Error	1	0.0260	0.0260	0.0260		
Total	8	59.0822				

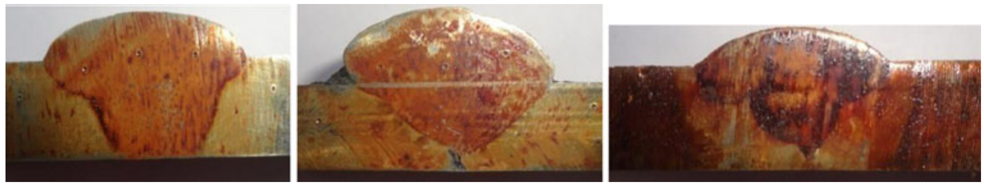

Fig. 7 Appearance of different weld bead geometry obtained on various samples

the most critical parameter which is also clear from response table of means. The tensile strength goes on increasing significantly as the welding current increases and the highest strength reported is at the higher value of welding current. The tensile strength also increases as the voltage goes on increasing. Welding speed has not affected the strength much, whereas the wire feed has shown abrupt variation in strength starting from less strength at low level of wire feed rate, then increases suddenly and decreases further as the wire feed rate goes on increasing.

The estimated coefficients for tensile strength are obtained by response surface modelling and a full quadratic equation is obtained for the tensile strength and is given in coded form below by Eq. 7:

$$\begin{aligned}\text{Tensile strength} = {} & 860.333 + 49.00(\mathrm{I}) + 30.333(\mathrm{V}) \\ & - 1.5(\mathrm{S}) + 21.167(\mathrm{F}) + 3.667(\mathrm{I})^2 \\ & - 0.333(\mathrm{V})^2 - 25.833(\mathrm{S})^2 \\ & - 67.833(\mathrm{F})^2 \end{aligned} \tag{7}$$

The equation in the uncoded form for weld tensile strength is given by Eq. 8.

$$\begin{aligned}\text{Tensile strength} = {} & -1148.73 - 0.1934(\mathrm{I}) \\ & + 20.1667(\mathrm{V}) + 9.5(\mathrm{S}) \\ & + 9.774(\mathrm{F}) + 0.001467(\mathrm{I})^2 \\ & - 0.0834(\mathrm{V})^2 - 0.4037(\mathrm{S})^2 \\ & - 0.01885(\mathrm{F})^2 \end{aligned} \tag{8}$$

The R^2 value obtained for the model is 91.16 %. The model for tensile strength either in coded form or in the uncoded form can be used to predict the tensile strength using different combinations of input variables.

3.5 Effect of process parameters on weld hardness

During the welding process, the hardness of material varies throughout the material. This is because large amount of heat is generated at the welding region and this heat is dissipated through the material to other areas. Even though welding is not carried at the other portion, its properties gets affected due to the heat dissipation, which is referred as heat affected zone. This effect can be normalised by giving heat treatment to the entire plate, which helps to improve and maintain the mechanical properties of material. In the present work also, all the test samples are given post-weld heat treatment. The hardness of all the samples is measured at various points of the weld joint using Rockwell hardness tester and the average hardness obtained for all the samples is given in Table 14.

The hardness for heat-treated Cr–Mo–V steel normally lies in the range of 10–36 Rc [27]. In the present work also, the hardness obtained is consistently above 30 Rc in most of the cases which is a good indication. The hardness obtained for each experiment is analysed to check the effect of each variable on the hardness. Figure 11 shows the effect of variables on the weld hardness whereas Table 15 gives the response table for means of weld hardness.

Table 10 Average weld penetration obtained in different experiments

Expt no.	*I* (Amp)	*V* (volts)	*S* (cm/min)	*F* (cm/min)	Weld penetration (mm)
1	350	28	4	190	6.27
2	350	30	12	250	11.00
3	350	32	20	310	6.65
4	400	28	12	310	8.69
5	400	30	20	190	11.00
6	400	32	4	250	8.03
7	450	28	20	250	9.20
8	450	30	4	310	11.00
9	450	32	12	190	9.94

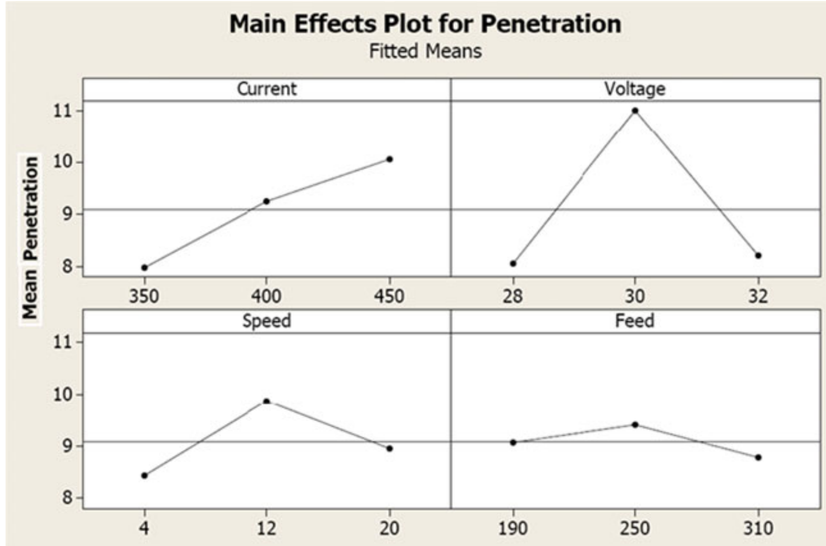

Fig. 8 Effect of input process variables on weld penetration

As there should be maximum hardness in the material, hence larger-the-better approach is considered to carry out the analysis of weld hardness. It is observed that the welding current is the most significant variable which affects the hardness much. For the lower level of welding current, the hardness obtained is maximum in the range of 35 Rc, then it is decreased suddenly up to 30 Rc as the welding current increases up to 400 Amp. The hardness increases again as the welding current further increases above 400 Amp. In case of voltage, maximum hardness is reported at the lower and higher levels of welding current whereas welding speed and wire feed have shown comparatively negligible effect on the weld hardness.

The estimated coefficients for hardness are obtained by response surface modelling and the full quadratic equation is obtained for the weld hardness. Equation 9 shows the weld hardness model in the coded form whereas the model in uncoded form is given by Eq. 10.

$$\text{Weld hardness} = 28.6667 - 0.8333(\text{I}) - 0.001(\text{V}) - 0.3333(\text{S}) + 0.3333(\text{F}) + 4.5(\text{I})^2 + 2.0(\text{V})^2 \quad (9)$$

Table 11 Response table for means for weld penetration

Level	Mean weld penetration (mm)			
	I	*V*	*S*	*F*
−1	7.973	8.053	8.433	9.070
0	9.240	11.00	9.877	9.410
+1	10.04	8.207	8.950	8.780
Delta	2.067	2.947	1.443	0.630
Rank	2	1	3	4

$$\text{Weld hardness} = 772.444 - 1.45667(\text{I}) - 30(\text{V}) - 0.04167(\text{S}) + 0.00556(\text{F}) + 0.0018(\text{I})^2 + 0.5(\text{V})^2 \quad (10)$$

The various combinations of models are attempted for hardness such as linear model, linear model with interaction effects, full quadratic model, etc. However the highest R^2 value of 81.07 % is obtained for full quadratic model. Thus Eq. (9) in coded form or Eq. (10) in uncoded form can be used to predict the hardness using different combinations of input variables.

The submerged arc welding of all the Cr–Mo–V steel samples is carried out and the analysis shows the effect of various input variables on the respective responses. The models developed are verified by conducting few more experiments and hence all the five models developed for the responses will be useful for predicting the output responses for the given set of input variables.

Fig. 9 Test sample no. 9 before and after test

Table 12 Tensile strength obtained during different experiments

Expt no.	*I* (Amp)	*V* (volts)	*S* (cm/min)	*F* (cm/min)	Tensile strength (MPa)
1	350	28	4	190	671
2	350	30	12	250	815
3	350	32	20	310	771
4	400	28	12	310	783
5	400	30	20	190	744
6	400	32	4	250	866
7	450	28	20	250	855
8	450	30	4	310	842
9	450	32	12	190	854

Table 13 Response table for means for weld tensile strength

Level	Mean weld tensile strength (MPa)			
	I	*V*	*S*	*F*
−1	752.3	769.7	793.0	756.3
0	797.7	800.3	817.3	845.3
+1	850.3	830.3	790.0	798.7
Delta	98.0	60.7	27.3	89.0
Rank	1	3	4	2

4 Parameters optimization using TLBO algorithm

The results obtained from the nine sets of experiments are carefully analysed and it is observed that a particular set of experiment having welding current=400 Amp, voltage=30 V, welding speed=20 cm/min, and wire feed rate=190 cm/min satisfies simultaneously all the three output responses related the weld bead geometry, i.e. this set of input parameters gives a minimum weld bead width of 18.502 mm, minimum weld reinforcement of 0.256 mm and maximum penetration of 11 mm. However, for the same set of input process parameters, the other two output responses are not optimum.

Hence in the present work, attempt is carried out to obtain an individual set of input process parameter which gives the optimum value of respective response. Attempt is also made to satisfy all the five output responses simultaneously by a single set of input process parameter. To achieve this target, a recently developed advanced optimization algorithm named as teaching–learning-based optimization algorithm (TLBO) is used [28, 29]. TLBO algorithm does not require any algorithm-specific parameters and only require the common control parameters like population size and number of iteration. It is already tested on various standard benchmark functions and its results are proved better than the other advanced optimization techniques [30]. Hence, attempt is made here to use the TLBO algorithm for the parameters optimization of the SAW process under consideration.

4.1 Optimum parameters setting for individual response

The various responses considered in the present work are conflicting in nature, i.e. weld bead width and weld reinforcement are need to be minimised whereas remaining responses are to be maximised. Hence in this section, each response is considered separately and attempted using the TLBO algorithm. A common population size of 20 is used and the number of generations considered is 30 which give a very consistent result for all the cases. The optimum

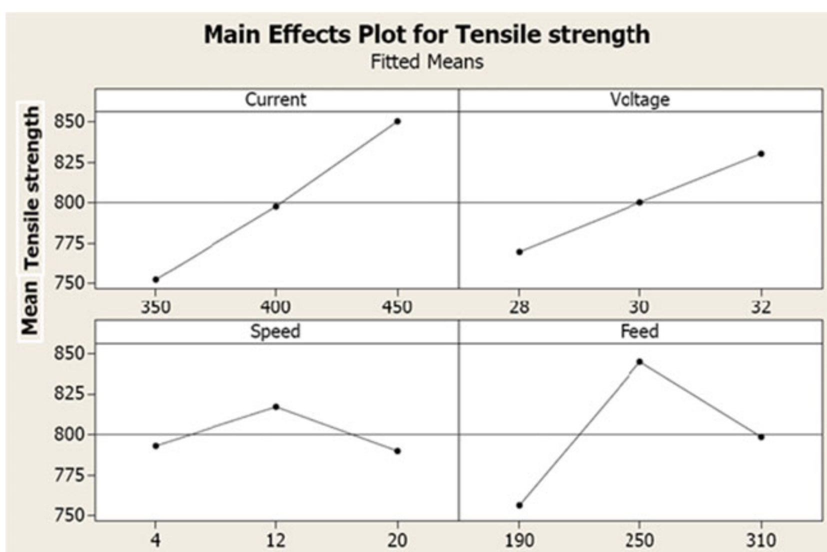

Fig. 10 Effect of input process variables on tensile strength

Table 14 Average weld hardness obtained during different experiments

Expt No.	*I* (Amp)	*V* (Volts)	*S* (cm/min)	*F* (cm/min)	Weld hardness (Rc)
1	350	28	4	190	36
2	350	30	12	250	34
3	350	32	20	310	36
4	400	28	12	310	31
5	400	30	20	190	28
6	400	32	4	250	31
7	450	28	20	250	34
8	450	30	4	310	33
9	450	32	12	190	34

parameter setting obtained for each response using TLBO algorithm is given in Table 16.

Certain conditions are kept while preparing the algorithm of some cases. For example, the case of weld reinforcement is of minimisation type. Hence, while attempting the algorithm, certain parameter setting may show the reinforcement less than 0 mm which is not justified because the reinforcement must be at least up to the upper edge of the joint which cause the joining of filler material with the base metal up to the face of the weld joint. Hence, appropriate care is taken while preparing the program so that the minimum reinforcement should not be less than 0 mm. Hence in the present case also, the optimum parameter setting for weld reinforcement gives the minimum reinforcement of 0.0086 mm.

Similarly, while attempting the maximisation of weld penetration, care is to be taken that the total thickness of weld plate is 11 mm. Hence, in the present work, the maximum allowed penetration is kept as 11.5 mm which can be justified also, because, even if more penetration is obtained below the root gap, it needed to be removed by grinding in order to have smooth functioning of the weld joint.

The parameter setting shown in Table 16 for each response optimises only the respective response and the remaining responses may not be optimum with the same setting. Hence, this parameter setting is to be used only when a certain response is of prime importance. In the next section, efforts are made to obtain a common process parameter setting which can satisfy all the objectives simultaneously.

4.2 Optimum parameters setting for combined objectives

In order to attempt all the objectives simultaneously, a normalised combined objective function is prepared as given by Eq. 11.

$$\begin{aligned}\mathrm{Min}\,Z = {} & W_1 \times (BW/BW_{min}) + W_2 \times (R/R_{min}) \\ & - W_3 \times (P/P_{max}) - W_4 \times (TS/TS_{max}) \\ & - W_5 \times (H/H_{max}) \qquad (11)\end{aligned}$$

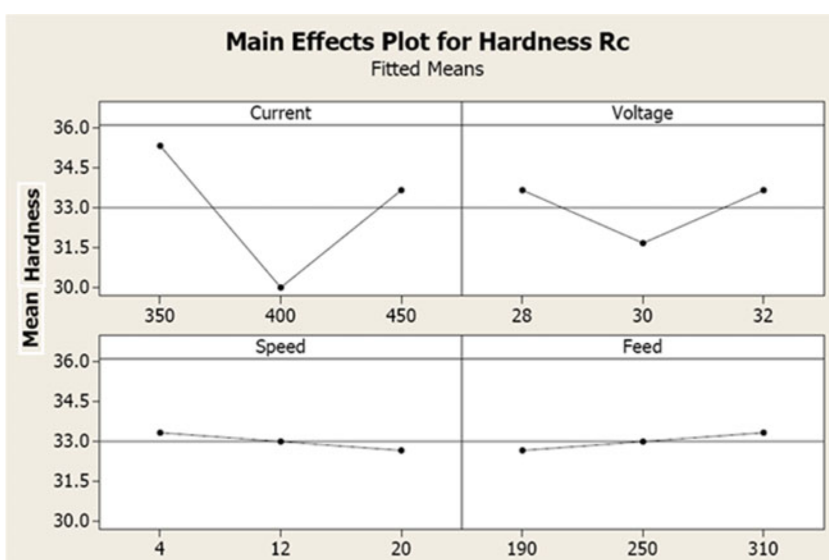

Fig. 11 Effect of each variable on weld hardness

Table 15 Response table for means of weld hardness

Level	Mean weld hardness (Rc)			
	I	*V*	*S*	*F*
−1	35.33	33.67	33.33	32.67
0	30.00	31.67	33.00	33.00
+1	33.67	33.67	32.67	33.33
Delta	5.33	2.00	0.67	0.67
Rank	1	2	3.5	3.5

Where, W_1, W_2, W_3, W_4 and W_5 are the weightages assigned to individual objective functions of weld bead width (BW), weld reinforcement (*R*), weld penetration (*P*), weld tensile strength (TS) and hardness (*H*), respectively. The weightages should be decided in such a way that addition of all the weightages becomes 1. In Eq. 11, BW_{min} and R_{min} are the minimum response reported by the respective models of weld bead width and weld reinforcement when these objectives are attempted separately. Similarly, P_{max}, TS_{max} and H_{max} are the maximum responses reported by the respective models of weld penetration, weld tensile strength and weld hardness when these objectives are attempted separately.

For deciding the various weightages used in Eq. 11, several combinations are tried by varying each weights in the range of 0.1–0.5 while maintaining the sum of total weights as 1. The different combination of weights reflects the optimised value of a particular objective whereas compromised values of remaining objectives are obtained. Hence, for such cases, the decision maker has to decide the importance of certain objectives and accordingly the weightages need to be decided.

Hence, one such compromised result is presented in the present work which is obtained by assigning equal weightage of 0.2 each to all the individual objective functions. The common parameters setting obtained by applying TLBO algorithm to the combined objective function is welding current=445 Amp, voltage=32 V, welding speed=7 cm/min, and wire feed rate=193 cm/min. This parameters setting nearly satisfies all the objectives and gives the minimum weld bead width of 27.05 mm, minimum weld reinforcement of 0.826 mm, maximum penetration of 9.32 mm, maximum tensile strength of 846.6 MPa and maximum hardness of 33.45 Rc. The optimum result obtained by using the combined objective function always gives the compromising result which may be different than the result of individual function value. The result produced above for the combined objective function is for the demonstration purpose; however, if any particular objective is very critical in decision making, then the respective weightage may be varied accordingly to obtain the optimum parameter setting.

5 Conclusion

Detailed experimental analysis is presented in the present work for submerged arc welding of Cr–Mo–V steel. Taguchi's L_9 orthogonal array is used for design of experiments and all the experiments are carried out on a 11-mm-thick Cr–Mo–V steel plate. Various important responses like weld bead width, weld reinforcement, weld penetration, weld tensile strength and weld hardness are measured in each experiment using sophisticated instruments and the results are analysed to study the effect of each input variable on the output responses. Appearance of weld bead geometry for all the welded samples along the cross-section are observed as considerably good and the tensile strength and hardness of the weldments are also on higher side which give a very strong weld joint. Response surface modelling is also carried out for each response and the models are developed for all the responses. The coefficients of determination obtained for all the cases are above 80 % and it is almost 100 % in the case of weld reinforcement. Optimised parameter setting is also obtained for each response using the TLBO algorithm. A combined objective function is also developed which can be used to obtain the common parameter setting which satisfies all the objectives simultaneously. The models developed for various output responses will be very useful for predicting the responses for the given sets of input variables of the submerged arc welding process.

Table 16 Optimum parameter setting for each response

Objective	*I* (Amp)	*V* (volts)	*S* (cm/min)	*F* (cm/min)	Optimum result
Minimum weld bead width	412	29	20	228	17.11 mm
Minimum weld reinforcement	378	31	18	214	0.0086 mm
Maximum weld penetration	444	29	5	241	11.16 mm
Maximum weld tensile strength	448	32	11	253	940.90 MPa
Maximum weld hardness	350	28	4	307	36.65 Rc

Acknowledgments The authors are thankful to the Gujarat Council on Science and Technology (GUJCOST), Gandhinagar, India for financial support to carry out the research work as a part of a project.

References

1. Swindeman RW, Santella ML, Maziasz PJ, Roberts BW, Coleman K (2004) Issues in replacing Cr–Mo steels and stainless steels with 9Cr–1Mo–V steel. Int J Press Vessel Pip 81:507–512
2. Lu SP, Kwon OY, Kim TB, Kim KH (2004) Microstructure and wear property of Fe–Mn–Cr–Mo–V alloy cladding by submerged arc welding. J Mater Process Technol 147:191–196
3. Storesund J, Borggreen K, Zang W (2006) Creep behaviour and lifetime of large welds in X 20 Cr-Mo-V 12 1—results based on simulation and inspection. Int J Press Vessel Pip 83:875–883
4. Zielinski A, Dobrzanski J, Krzton H (2007) Structural changes in low alloy cast steel Cr–Mo–V after long time creep service. J Achiev Mater Manuf Eng 25:33–36
5. Prasad K, Dwivedi DK (2008) Some investigations on microstructure and mechanical properties of submerged arc welded HSLA steel joints. Int J Adv Manuf Technol 36:475–483
6. Hilkes J, Gross V (2009) Welding Cr–Mo steel for power generation and petrochemical application—past, present and future. IIW Conference, Singapore, pp 1–11
7. Naz N, Tariq F, Baloch RA (2009) Failure analysis of HAZ cracking in low C–CrMoV steel weldment. J Fail Anal Prev 9:370–379
8. Arivazhagan B, Prabhu R, Albert SK, Kamaraj M, Sundaresan S (2009) Microstructure and mechanical properties of 9Cr-1Mo steel weld fusion zones as a function of weld metal composition. J Mater Eng Perform 18:999–1004
9. Babu SPK, Natarajan S (2010) High temperature corrosion and characterization studies in flux cored arc welded 2.25Cr-1Mo power plant steel. J Mater Eng Perform 19:743–750
10. Murugan N, Parmar RS, Sud SK (1993) Effect of submerged arc welding process variables on dilution and bead geometry in single wire surfacing. J Mater Process Technol 37:767–780
11. Chandel RS, Seowl HP, Cheong FL (1997) Effect of increasing deposition rate on the bead geometry of submerged arc welds. J Mater Process Technol 72:124–128
12. Chandel RS (1998) The effect of process variables on the flux consumption in submerged arc welding. Mater Manuf Process 13(2):181–188
13. Brito VLO, Voorwald HJC, Neves N, Bott IS (2001) Effects of a postweld heat treatment on a submerged arc welded ASTM A537 pressure vessel steel. J Mater Eng Perform 10:249–257
14. Sharma A, Arora N, Mishra BK (2008) A practical approach towards mathematical modelling of deposition rate during twin-wire submerged arc welding. Int J Adv Manuf Technol 36:463–474
15. Bang K, Park C, Jung H, Lee J (2009) Effects of flux composition on the element transfer and mechanical properties of weld metal in submerged arc welding. Met Mater Int 15(3):471–477
16. Tsai HL, Tarng YS, Tseng CM (1996) Optimization of submerged arc welding process parameters in hardfacing. Int J Adv Manuf Technol l2:402–406
17. Gunaraj V, Murugan N (2000) Prediction and optimization of weld bead volume for the submerged arc process-part 2. Weld J Res Suppl 331–338
18. Murugan N, Gunaraj V (2005) Prediction and control of weld bead geometry and shape relationships in submerged arc welding of pipes. J Mater Process Technol 168:478–487
19. Dhas JER, Kumanan S (2011) Optimization of parameters of submerged arc weld using non conventional techniques. Appl Soft Comput 11(8):5198–5204
20. Gowtham KM, Vasudevan M, Maduraimuthu V, Jayakumar T (2011) Intelligent modeling combining adaptive neuro fuzzy inference system and genetic algorithm for optimizing welding process parameters. Metall Mater Trans B 42B:385–392
21. Tarng YS, Yang WH (1998) Application of the Taguchi method to the optimization of the submerged arc welding process. Mater Manuf Process 13:455–467
22. Tarng YS, Yang WH, Juang SC (2000) The use of fuzzy logic in the Taguchi method for the optimisation of the submerged arc welding process. Int J Adv Manuf Technol 16:688–694
23. Tarng YS, Juang SC, Chang CH (2002) The use of grey-based Taguchi methods to determine submerged arc welding process parameters in hardfacing. J Mater Process Technol 128:1–6
24. Datta S, Bandyopadhyay A, Pal PK (2008) Application of Taguchi philosophy for parametric optimization of bead geometry and HAZ width in submerged arc welding using a mixture of fresh flux and fused flux. Int J Adv Manuf Technol 36:689–698
25. Datta S, Bandyopadhyay A, Pal PK (2008) Grey-based Taguchi method for optimization of bead geometry in submerged arc bead-on-plate welding. Int J Adv Manuf Technol 39:1136–1143
26. Aeronautical Research Council (1964) The chemical contouring of 3% chromium–molybdenum–vanadium and 5% chromium–molybdenum–vanadium high strength steel sheet. Bristol Aerojet Ltd, London. C.P. No.811
27. Viswanathan R, Shaw BJ (1974) Effect of heat treatment on temper embrittlement susceptivility of Cr-Mo-V steels. Scr Metall 8(11):1255–1260
28. Rao RV, Savsani VJ, Vakharia DP (2011) Teaching–learning-based optimization: a novel method for constrained mechanical design optimization problems. Comp-Aided Design 43:303–315
29. Rao RV, Savsani VJ, Vakharia DP (2012) Teaching–learning-based optimization: an optimization method for continuous non-linear large scale problem. Inf Sci 183:1–15
30. Rao RV, Patel V (2012) An elitist teaching–learning-based optimization algorithm for solving complex constrained optimization problems. Int J Ind Eng Comput 3(4):535–560